REMOTELY SENSED AVALANCHE ACTIVITY DURING THREE EXTREME AVALANCHE PERIODS IN SWITZERLAND

Elisabeth D. Hafner[1,2,3,*], Frank Techel[1], Holger Heisig[4], Jor Fergus Dal[1,2], Yves Bühler[1,2]

[1] *WSL Institute for Snow and Avalanche Research SLF, Davos, Switzerland*
[2] *Climate Change, Extremes, and Natural Hazards in Alpine Regions Research Center CERC, Davos, Switzerland*
[3] *EcoVision Lab, Photogrammetry and Remote Sensing, ETH Zurich, Zurich, Switzerland*
[4] *Federal Office of Topography swisstopo, Wabern, Switzerland*

ABSTRACT:
Systematic mapping of avalanches using remote-sensing technologies has become a reliable and – when combined with machine-learning algorithms – also time-effective way to document avalanche activity over large areas. Making use of these technological advances, we compared the avalanche activity for three periods with widespread activity of very large and extremely large avalanches, when the highest danger level *5 (very high)* was forecast for large parts of the Swiss Alps. In these three periods (in 1999, 2018, 2019), avalanches were captured with different remote-sensing instruments: in 1999, with airplane imagery, in 2018 and 2019 with multispectral satellite data. Comparing the activity of all three periods to Large Scale Hazard Indication Modelling (LSHIM) of avalanches with a 100-year return period allowed to compare how much of the potential avalanche terrain was active and to quantitatively compare activity between these periods. We found that 19% of the avalanche release areas showed activity in 1999 compared to 16% in 2018 and 8% in 2019. Considering the avalanche area delimited using the 100-year return period, 17% were active in 1999, 11% in 2018 and 6% in 2019. By comparing the three avalanche periods, we contribute to better understand the extent and return periods of very large and extremely large avalanches (size 4 and 5) and demonstrate, how avalanche mapping from remotely sensed data can make avalanche databases more complete.

Keywords: avalanche mapping, potentially active area, danger level 5 (very high)

1. INTRODUCTION

Spatially continuous documentation of avalanche occurrences is important as knowing when, where, and under which conditions avalanches occurred is necessary to verify model simulations (i.e., for run-out or return periods of avalanches), public avalanche forecasts or avalanche hazard zoning, or to permit targeted planning of risk mitigation measures. However, today, data on avalanche occurrence is still often limited to specific locations or situations.

For decades, acquisition of avalanche occurrence data have relied solely on human observers. More recently it has been complemented by stationary sensors like Doppler radars or infra-sound systems (e.g., Schimmel et al., 2017), and remote sensing with satellites, airplanes or drones (e.g., Lato et al., 2012; Eckerstorfer et al., 2016; Hafner et al., 2021, 2023). Both optical and synthetic aperture radar (SAR) satellite data have been successfully used to systematically and automatically map avalanches over large areas (Bühler et al., 2019; Hafner et al., 2022; Eckerstorfer et al., 2019; Bianchi et al., 2021).

Relying on large-scale documentation of avalanches using remote sensing, we analyze avalanche activity for three periods with widespread activity of very large (size 4) and extremely large (size 5) avalanches in Switzerland (1999, 2018, 2019), with a particular focus on avalanche activity in the Canton of Grisons in Eastern Switzerland. We describe and compare avalanche activity during these three extreme avalanche periods with the objective to (1) understand large-scale activity patterns, (2) quantify the active area relative to the Large Scale Hazard Indication Modelling (LSHIM), and (3) compare detected avalanches with the LSHIM to estimate the quality of the LSHIM approach.

2. DATA AND METHODS

2.1 Avalanche periods and avalanche documentation

Since the late 1990's, Switzerland had three periods when danger level *5 (very high)* was issued. The first and longest period occurred in January and February 1999 (EISLF, 2000; Wilhelm et al., 2000), while the other two occurred in January 2018 and 2019 (hereafter called 1999, 2018 and 2019; Bründl et al., 2019; Bühler et al., 2019; Zweifel et al., 2019). All three were characterized by large amounts of new snow accompanied by strong winds

*Corresponding author address:
Elisabeth D. Hafner
WSL Institute for Snow and Avalanche Research
Flüelastrasse 11, 7260 Davos Dorf, Switzerland
tel: +41 81 4170 359
email: elisabeth.hafner@slf.ch or elisabeth_hafner@bluewin.ch

from north to west, leading to intense avalanche activity (EAWS, 2024a, Tab. 1). While the periods in 1999 and 2018 had varying air temperature with intermittent rain to higher elevation (EISLF, 2000; Bründl et al., 2019), January 2019 had the coldest temperatures measured compared to the preceding 30 years (Zweifel et al., 2019).
Optical imagery was acquired for all three periods to document the avalanche activity: in 1999, the Federal Office of Topography (swisstopo) acquired panchromatic aerial imagery[1] with a scale of 1:30'000 between 25 February and 1 March. The data were orthorectified and processed to 0.5 m in 2023 with the methodology described in Heisig and Simmen (2021). In 2018 and 2019 optical SPOT6/7[2] data were acquired through the Swiss rapid mapping chain (Bühler et al., 2019) with a spatial resolution of 1.5 m and information in the channels red, green, blue and near-infrared (RGB, NIR) for approximately 12'500 km^2 in 2018 (24.1.2018; Bühler et al., 2019) and 9'500 km^2 in 2019 (16.1.2019; Zweifel et al., 2019).

2.2 Avalanche mappings

For 1999, a combination of manual mapping and automatic identification with deep learning (for details see Dal et al., 2024) followed by manual corrections, was used to map all visible avalanches. The manual mapping and the corrections were aided by the Swiss national topographic map (Swiss Map; swisstopo, 2020a), a summer orthophoto mosaic (SWISSIMAGE; swisstopo, 2020b) and the slope angle calculated from the Swiss national DTM (swissALTI3D; swisstopo, 2018). At the time of writing, the manual validation of the automatically identified and delineated avalanches are still in progress; currently 3'900 avalanches have been mapped (Fig. 1).
From the SPOT6/7 data, avalanches were identified and manually digitized as polygons (for details on the methodology see Bühler et al., 2019). Over Switzerland 18'737 avalanches were mapped in 2018 and 6'041 in 2019 (Fig. 1). The completeness of the 2018 and 2019 data were investigated in Hafner et al. (2021) and the avalanches have been used to train a deep learning model to automate the mapping procedure (Hafner et al., 2022).

2.3 Large Scale Hazard Indication Modelling (LSHIM)

In Switzerland, municipalities are mandated to develop hazard maps and incorporate hazard zones (white, blue, red zones) into spatial planning (ForA, 1991). Hazard maps are required for settlements and areas with significant infrastructure, which in the

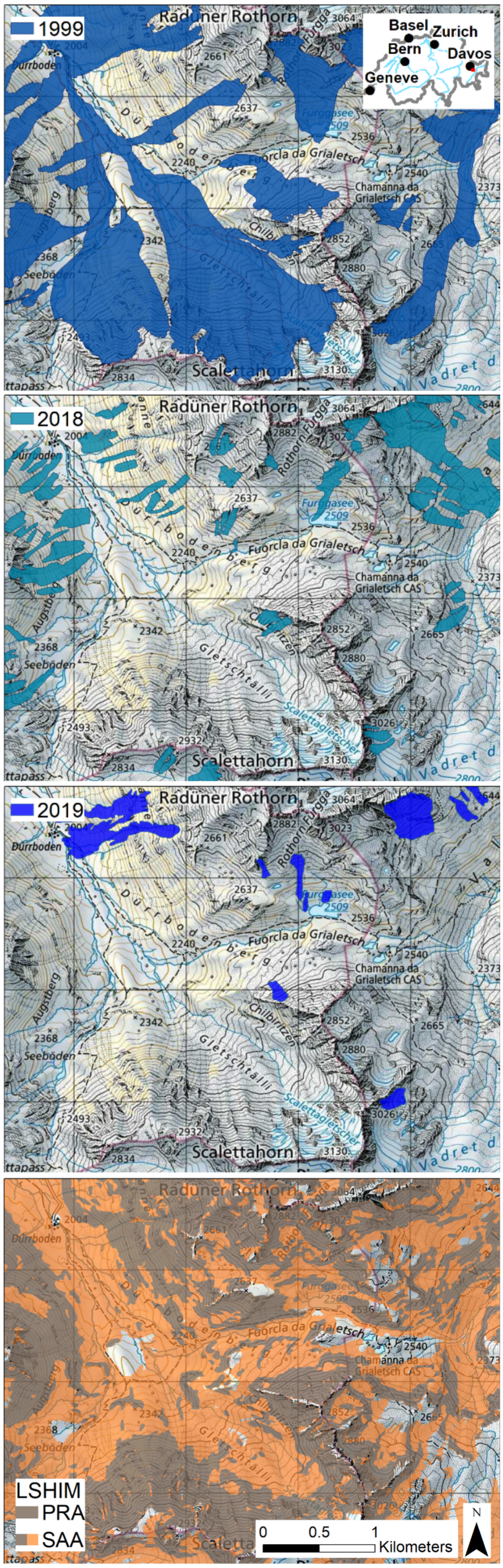

Figure 1: Example of the mapped avalanches from the three avalanche periods and the corresponding Large Scale Hazard Indication Modelling (LSHIM) in the Dischma valley, Davos, Switzerland (map source: Federal Office of Topography).

[1]Leica RC30 camera
[2]SPOT - Satellite pour l'Observation de la Terre

Table 1: Comparison of conditions for the three avalanche periods with danger *5 (very high)*. The avalanches observed refer to point observations and mappings from observers in the field.

year	duration	max. new snow [m]	level 5 [days]	extent level 5 [km^2]	destructive avalanches*	avalanches mapped GR	avalanches observed GR
1999	27.01.1999-25.02.1999	5 - 7 (27 days)	6	≈ 19'500	1'200**	3'020	521
2018	26.12.2017-23.01.2018	4 - 5 (27 days)	4	10'401	141	6'998	818
2019	09.01.2019-15.01.2019	2 - 3 (10 days)	1	5'109	144	3'878	435

*whole Switzerland, **whole winter, GR = Canton Grisons

case of the Canton of Grisons means approximately 10% of the area.

Over the past decade, the WSL Institute for Snow and Avalanche Research SLF (SLF) developed the Large Scale Hazard Indication Modelling (LSHIM; Bühler et al., 2018a, 2022) approach, in close collaboration with cantonal experts. LSHIM automatically delineates potential avalanche release areas (PRAs; Bühler et al., 2013, 2018b), simulates them with the numerical avalanche simulation software RAMMS (Christen et al., 2010) and therefore allows assessing avalanche danger in areas outside the official hazard maps.

LSHIM is simulated for 10-, 30-, 100- and 300-year return periods, keeping the approach as close as possible to the Swiss guidelines for hazard mapping (Margreth, 2019). For this study, we applied the 100-year scenario, as we deemed this the most suitable for the three extreme avalanche periods (Fig. 1; EISLF, 2000; Bründl et al., 2019; Zweifel et al., 2019). From these scenarios, we extracted the potential release areas (PRAs) and the simulated avalanche affected area (SAA; PRAs with associated runouts ≥1kPa).

2.4 Analysis

We laid a 1x1 km grid over the canton of Grisons and kept only cells where optical data were available for the full grid cell (Tab. 2). The area classified as PRA and SAA was calculated based on LSHIM simulations. These values characterize each grid cell or aggregate of grid cells with regard to potential avalanche affected area. We then calculated the proportion of PRA and SAA, which were active, where *active* is defined as the overlap between mapped avalanches and PRA/SAA (Fig. 2). We analyzed the share of active cells, share of cells with ≥50% activity, and the maximum observed activity per cell. In addition, we compared the activity in more detail for the 1'049 km^2 where data were available for all three avalanche periods. Lastly, we computed the share of mapped avalanche area outside the LSHIM and analyzed the validity of the modelling.

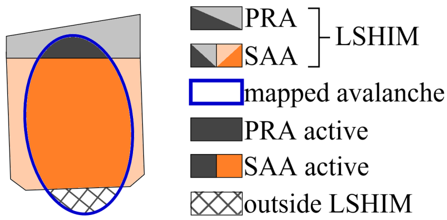

Figure 2: Illustration of the Large Scale Hazard Indication Modelling (LSHIM) divided into potential release area (PRA) and simulated avalanche area (SAA), the mapped avalanches, the resulting active area as well as avalanche area outside the LSHIM.

3. RESULTS

The documented (mapped) avalanche area was the most extensive in 1999 (186.5 km^2), despite the area coverage being the smallest of the three periods (Tab. 2). In 1999, the mapped avalanche area was 35 to 50 km^2 more than in the other two periods. Comparing the LSHIM with the avalanche mappings, we found the highest activity for 1999 with 19% of the PRAs and 17% of the SAA active (Tab. 2). In 2018, the share of active PRAs (SAA) was 3% (6%) lower than 1999, but double that of 2019. The spatial distribution of hot spots with increased avalanche activity showed similar patterns across the three avalanche periods, though the magnitude varied (see Fig. 3). Regions with a high number of active PRAs did not always align with a significant proportion of active SAAs (Fig. 3). When comparing the three periods on the overlapping subset (1'049 km^2), 1999 was again the most active with around 70% (partially) active grid cells, both for PRA and SAA (Tab. 3 and 4). In 2018 about two thirds of all grid cells with PRA or SAA showed (some) activity, while in 2019 less than half of all cells showed activity. The area active varied in the active cells, in 1999 6.8% of all cells had above or equal to 50% of the PRA active (Tab. 3). This is more than double compared to 2018 and about ten times more than in 2019. When analyzing the SAA, we found a similar pattern: in 1999, 6.4% of all possible cells showed greater or equal to 50% activity. The other two periods had again less grid cells with this much activity (2018: 1.7%; 2019: 0.4%).

Table 2: Comparison of the mappings from the three avalanche periods in the canton of Grisons to the Large Scale Hazard Indication Modelling (LSHIM). The LSHIM was divided into potential release area (PRA) and simulated avalanche area (SAA).

period	area [km^2]	avalanche area* [km^2]	outside LSHIM* [%]	PRA [km^2]	PRA active [%]	SAA [km^2]	SAA active [%]
1999	1'654	186.5	2.0	514.5	19	1092.7	17
2018	2'067	136.7	1.9	516.7	16	1'185.7	11
2019	4'394	149.8	1.4	1'153.9	8	2'521.9	6

*considering only avalanches in fully covered grid cells

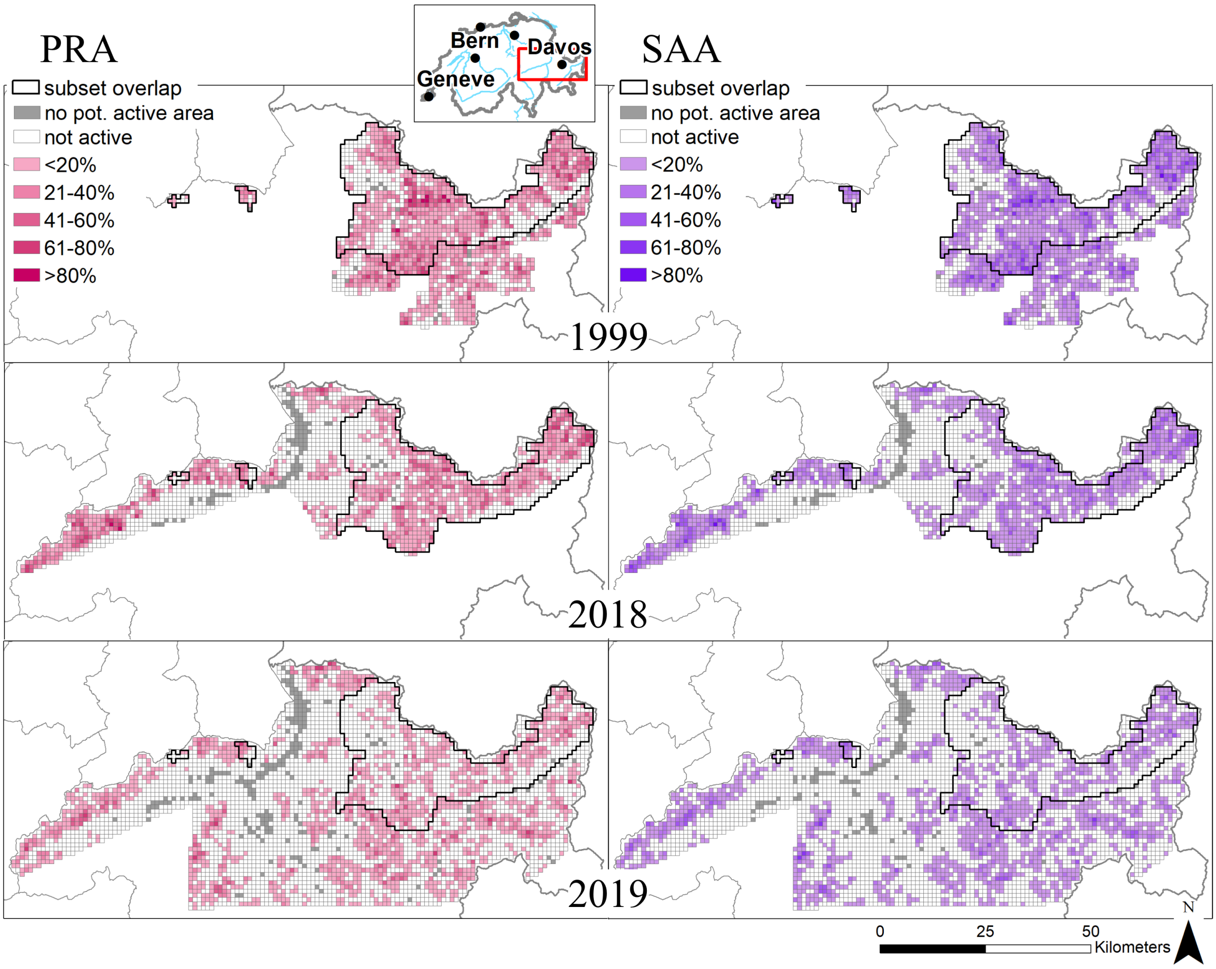

Figure 3: Area active in the three avalanche periods compared to the delineated potential avalanche release area (PRA) and the simulated avalanche area (SAA). The black line frames the area with data from all three avalanche periods.

Table 3: Comparison between the potential release areas (PRA) and the mapped avalanches for area covered in all three years (1'049 km^2).

period	cells with PRA [km^2]	active PRA cells [%]	cells ≥50% active PRA [%]	PRA [km^2]	mean PRA active [%/ cell]	max. PRA active [%/ cell]
1999		69	6.8		15	97
2018	1039	61	2.8	313	11	72
2019		44	0.7		5	64

The highest percentage of active PRA in one grid cell amounted to 97% and was found in 1999 (Tab. 3 and Fig. 4). The maximum SAA active per grid cell was 85% and was also recorded in 1999. The maximum values for 2018 and 2019 were between 24 and 33% lower (Tab. 4 and Fig. 4). The share of area outside the LSHIM was between 1.4 and 2% of the total avalanche area per period. These areas were primarily located in flat runout areas and in very steep starting zones (Tab. 2).

Table 4: Comparison between the simulated avalanche area (SAA) and mapped avalanches for area covered in all three years (1'049 km^2).

period	cells with SAA [km^2]	active SAA cells [%]	cells ≥50% active SAA [%]	SAA [km^2]	mean SAA active [%/ cell]	max. SAA active [%/ cell]
1999	1043	73	6.4	701	15	85
2018		63	1.7		9	61
2019		47	0.4		4	58

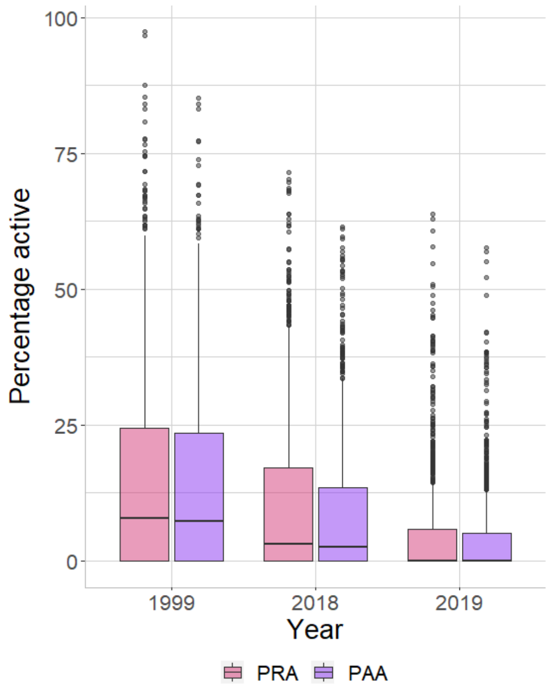

Figure 4: Distribution of active potential release area (PRA) and active simulated avalanche area (SAA) for the grid cells mapped in all three avalanche periods.

4. DISCUSSION

We explored avalanche activity patterns for three extreme avalanche periods. The key findings were as follows:

- hot spots with higher avalanche activity showed similar patterns, but varying magnitude between the three avalanche periods,
- in comparison, 1999 had the highest share of both PRA and SAA active with 15% each, and
- 2% or less of the mapped avalanche area were located outside the LSHIM 100y scenario.

4.1 Benefits of large-scale mappings

Relying on remote sensing, avalanche periods can be documented reliably covering large regions. For the three avalanche periods investigated, the mappings from remotely sensed imagery included six to nine times more avalanche observations than traditional observation methods (Tab. 1). Avalanche documentation is certainly not complete using this approach. Nonetheless it significantly expands the information available for hazard mapping, planning and evaluation of mitigation measures, risk analysis, verification of avalanche forecasts, and validation of avalanche simulations, all of which rely on data from past events. Moreover, comprehensive inventories over large areas enable continuous analyses and reveal differences and similarities in large-scale avalanche activity patterns.

4.2 Limitations

Avalanche activity was markedly the highest for 1999, when the active avalanche area was 4 times that of 2018 and 17 times that of 2019. The difference in activity is also in line with the number of days for which danger level *5 (very high)* was forecast: in 1999 there were 1.5 times more days than 2018 (6 vs. 4) and six times more than 2019 (6 vs. 1). Records of observed avalanches in existing databases and documented destructive avalanches, both independent of our analysis, confirm these differences between the periods (Tab. 1).

Though these differences seem plausible, differing image acquisition methodologies may also impact the completeness of avalanche records, leading to observed differences between the years as image acquisition methodologies differ. For instance, avalanche records obtained from SPOT6/7 imagery are less complete in shaded compared to illuminated areas (Hafner et al., 2021). In contrast, acquisition parameters for the aerial imagery from 1999 were specifically adjusted for snow, leading to good visibility also in shaded areas. Additionally, avalanches with larger release heights and deposits, as was the case in 1999, can be recognized even after subsequent snowfalls, while smaller avalanches may not be visible anymore.

Avalanche mappings only capture the visible dense part of avalanches, while areas affected by powder snow avalanches cannot be detected on these images (except there was damage to forest). In 2019, many avalanches released as large powder snow avalanches, fuelled by the cold conditions. Hence, these avalanches are less reliably captured in the mapping and are also not accounted for in the LSHIM modelling, making a comparison difficult.

Hafner et al. (2023) showed large differences in avalanche area identified by different domain experts, relying on aerial and drone imagery. For a small subset of the underlying remotely sensed data, Dal et al. (2024) and Hafner et al. (2022) confirmed that our avalanche data were also affected. However, since all our avalanches were mapped, or manually corrected by the same person, we believe the effect on the comparison between the avalanche periods to be negligible.

4.3 Implications for avalanche forecasting

In Europe, the avalanche danger levels used in public avalanche forecasts are described by snowpack stability, the frequency distribution of snowpack stability, and avalanche size (EAWS, 2024b). Thus, for a specific region, avalanche forecasters are required to forecast the number of locations where avalanches could release (frequency of stability) given a certain load (stability). This frequency (or number) is described using natural-language expressions like *many*, *some*, *a few*, or *(nearly) none* (EAWS, 2024c). Definitions for these classes are purely descriptive, actual numbers describing these classes quantitatively are lacking. For instance, at danger level *5 (very high)*, *many* locations exist where natural avalanches may release (EAWS, 2024b).

The observed proportion of active release areas, as observed in this study, can provide an indication of what a term like *many* could mean in numbers. Even though we analyzed the three most extreme avalanche periods during the last 25 years, only between 8% and 19% of all PRAs were active (Tab. 2). This suggests that a term like *many* as used in the context of public avalanche forecasting includes conditions when avalanches may release in just a comparably small share of release areas within a region.

4.4 Validation of the LSHIM

The LSHIM approach was developed and tested in close collaboration with experts from the cantonal authorities. Nevertheless, its accuracy is limited due to the automated computer-based approach, applying digital terrain models (DTMs) and information on protective forest densities (Bühler et al., 2022). For example, in extreme avalanche events, delineated PRAs on large slopes are smaller than observed release areas. The LSHIM does not consider protection measures such as snow fences for the canton of Grisons. Measures such as deflecting and catching dams are not fully taken into account, as they are smoothed out by the resolution of the applied DTM. Only the dense flowing part of avalanches is simulated, but not the powder cloud. Furthermore the scenario (100 year return period in this case) is hard to estimate for real avalanche events. For selected avalanches in 1999, return periods larger than the modeled 100 years have been estimated (EISLF, 2000). With these limitations in mind, the result that only 2% of the simulated avalanche area is overrun by the mapped avalanches, confirms the overall validity of the LSHIM for hazard mapping though closer inspection of these areas is needed.

5. CONCLUSIONS AND OUTLOOK

Remote sensing based large-scale avalanche mappings allow a systematic documentation and analysis of avalanche activity, permitting for a first time a quantitative comparison of avalanche activity during three periods with extreme activity in Switzerland. By comparing mapped avalanches with large-scale hazard indication maps, we showed that even though danger level *5 (very high)* was forecast during all three periods, the area active varied. 1999 was by far the most active period, with 15% of the potential avalanche area active in the 1'049 km^2 covered in all years.

Our findings show that remote sensing based mappings in combination with LSHIM, though not free of error and uncertainty, paint a more complete picture of differences and similarities in avalanche activity. Overall the systematic mapping of avalanches is a unique opportunity to better understand avalanche activity patterns over large areas and to provide data on past avalanches for the relevant stakeholders.

With the mapping from 1999 still ongoing, the three avalanche periods may soon be compared over a larger part of Switzerland, enhancing the understanding of the avalanche activity during extreme periods. For future avalanche periods, systematic mappings from satellite or airplane imagery offer the unique opportunity to compare the activity over large areas. Documentation of more avalanche periods, also at lower danger levels, has the potential to enlarge understanding and help quantify, e.g., the frequency classes, like *many* or *some*, used for avalanche forecasting.

==

ACKNOWLEDGEMENTS

The authors thank the Federal Office for the Environment FOEN and the canton Valais for partially funding the SPOT6/7 data. We also thank the cantons Valais, Graubünden, Bern, Obwalden and Uri as well as Liechtenstein for partially funding the mapping of the 2018 and 2019 avalanches.

References

Bianchi, F. M., Grahn, J., Eckerstorfer, M., Malnes, E., and Vickers, H.: Snow Avalanche Segmentation in SAR Images With Fully Convolutional Neural Networks, IEEE Journal of Selected Topics in Applied Earth Observations and Remote Sensing, 14, 75–82, doi:10.1109/JSTARS.2020.3036914, 2021.

Bründl, M., Hafner, E., Bebi, P., Bühler, Y., Margreth, S., Marty, C., Schaer, M., Stoffel, L., Techel, F., Winkler, K., Zweifel, B., and Schweizer, J.: Ereignisanalyse Lawinensituation im Januar 2018, WSL Berichte, p. 162 p., URL https://www.dora.

lib4ri.ch/wsl/islandora/object/wsl:19842, last access: 2024-07-25, 2019.

Bühler, Y., Kumar, S., Veitinger, J., Christen, M., Stoffel, A., and Snehmani: Automated identification of potential snow avalanche release areas based on digital elevation models, Natural Hazards and Earth System Sciences, 13, 1321–1335, doi:10.5194/nhess-13-1321-2013, URL https://nhess.copernicus.org/articles/13/1321/2013/, 2013.

Bühler, Y., von Rickenbach, D., Christen, M., Margreth, S., Stoffel, L., and Stoffel, A.: Linking modeled potential release areas with avalanche dynamics simulations: an automated approach for efficient avalanche hazard indication mapping, in: International Snow Science Workshop Proceedings 2018, Innsbruck, Austria, pp. 810–814, URL https://arc.lib.montana.edu/snow-science/objects/ISSW2018_P08.22.pdf, last access: 2024-08-05, 2018a.

Bühler, Y., von Rickenbach, D., Stoffel, A., Margreth, S., Stoffel, L., and Christen, M.: Automated snow avalanche release area delineation – validation of existing algorithms and proposition of a new object-based approach for large-scale hazard indication mapping, Natural Hazards and Earth System Sciences, 18, 3235–3251, doi:10.5194/nhess-18-3235-2018, URL https://nhess.copernicus.org/articles/18/3235/2018/, 2018b.

Bühler, Y., Hafner, E. D., Zweifel, B., Zesiger, M., and Heisig, H.: Where are the avalanches? Rapid SPOT6 satellite data acquisition to map an extreme avalanche period over the Swiss Alps, The Cryosphere, 13, 3225–3238, doi:10.5194/tc-13-3225-2019, URL https://tc.copernicus.org/articles/13/3225/2019/, 2019.

Bühler, Y., Bebi, P., Christen, M., Margreth, S., Stoffel, L., Stoffel, A., Marty, C., Schmucki, G., Caviezel, A., Kühne, R., Wohlwend, S., and Bartelt, P.: Automated avalanche hazard indication mapping on a statewide scale, Natural Hazards and Earth System Sciences, 22, 1825–1843, doi:10.5194/nhess-22-1825-2022, URL https://nhess.copernicus.org/articles/22/1825/2022/, 2022.

Christen, M., Kowalski, J., and Bartelt, P.: RAMMS: Numerical simulation of dense snow avalanches in three-dimensional terrain, Cold Regions Science and Technology, 63, 1–14, doi:10.1016/j.coldregions.2010.04.005, 2010.

Dal, J. F., Hafner, E. D., Peters, T., Narnhofer, D., Daudt, R. C., Heisig, H., and Bühler, Y.: Automated snow avalanche mapping with deep learning in aerial imagery from the extreme avalanche winter of 1999, in: International Snow Science Workshop Proceedings 2024, Tromsø, Norway, 2024.

EAWS: Standards: Avalanche Danger Scale, URL https://www.avalanches.org/standards/avalanche-danger-scale/, last access: 2024-02-16, 2024a.

EAWS: EAWS Matrix, URL https://www.avalanches.org/standards/eaws-matrix/, last access: 2024-08-06, 2024b.

EAWS: Standards: Snowpack stability and frequency, URL https://www.avalanches.org/standards/snowpack-stability-frequency/, last access: 2024-08-12, 2024c.

Eckerstorfer, M., Bühler, Y., Frauenfelder, R., and Malnes, E.: Remote sensing of snow avalanches: Recent advances, potential, and limitations, Cold Regions Science and Technology, 121, 126–140, doi:10.1016/j.coldregions.2015.11.001, URL https://www.sciencedirect.com/science/article/pii/S0165232X15002591, 2016.

Eckerstorfer, M., Vickers, H., Malnes, E., and Grahn, J.: Near-Real Time Automatic Snow Avalanche Activity Monitoring System Using Sentinel-1 SAR Data in Norway, Remote Sensing, 11, doi:10.3390/rs11232863, URL https://www.mdpi.com/2072-4292/11/23/2863, 2019.

EISLF: Der Lawinenwinter 1999: Ereignisanalyse, Eidg. Institut für Schnee- und Lawinenforschung, URL https://www.dora.lib4ri.ch/wsl/islandora/object/wsl%3A17698, last access: 2024-07-25, 2000.

ForA: Federal Act on Forest of 4. October 1991 (Forest Act, ForA 1991, SR 921.0), The Federal Assembly of the Swiss Confederation, URL https://www.fedlex.admin.ch/eli/cc/1992/2521_2521_2521/en, last access: 2024-08-05, 1991.

Hafner, E. D., Techel, F., Leinss, S., and Bühler, Y.: Mapping avalanches with satellites – evaluation of performance and completeness, The Cryosphere, 15, 983–1004, doi:10.5194/tc-15-983-2021, URL https://tc.copernicus.org/articles/15/983/2021/, 2021.

Hafner, E. D., Barton, P., Daudt, R. C., Wegner, J. D., Schindler, K., and Bühler, Y.: Automated avalanche mapping from SPOT 6/7 satellite imagery with deep learning: results, evaluation, potential and limitations, The Cryosphere, 16, 3517–3530, doi:10.5194/tc-16-3517-2022, URL https://tc.copernicus.org/articles/16/3517/2022/, 2022.

Hafner, E. D., Techel, F., Daudt, R. C., Wegner, J. D., Schindler, K., and Bühler, Y.: Avalanche size estimation and avalanche outline determination by experts: reliability and implications for practice, Natural Hazards and Earth System Sciences, 23, 2895–2914, doi:10.5194/nhess-23-2895-2023, URL https://nhess.copernicus.org/articles/23/2895/2023/, 2023.

Heisig, H. and Simmen, J.-L.: Re-engineering the Past: Countrywide Geo-referencing of Archival Aerial Imagery, PFG – Journal of Photogrammetry, Remote Sensing and Geoinformation Science, 89, 487–503, doi:10.1007/s41064-021-00162-z, URL http://dx.doi.org/10.1007/s41064-021-00162-z, 2021.

Lato, M. J., Frauenfelder, R., and Bühler, Y.: Automated detection of snow avalanche deposits: Segmentation and classification of optical remote sensing imagery, Natural Hazards and Earth System Sciences, 12, 2893–2906, doi:10.5194/nhess-12-2893-2012, 2012.

Margreth, S.: Lawinengefahrenkarten in der Schweiz. Avalanche hazard maps in Switzerland, Wildbach- und Lawinenverbau, 83, 80–92, URL https://www.dora.lib4ri.ch/wsl/islandora/object/wsl%3A25901, last access: 2024-08-15, 2019.

Schimmel, A., Hübl, J., Koschuch, R., and Reiweger, I.: Automatic detection of avalanches: evaluation of three different approaches, Natural Hazards, 87, 83–102, doi:10.1007/s11069-017-2754-1, 2017.

swisstopo: swissALTI3D - Das hoch aufgelöste Terrainmodell der Schweiz, URL https://www.swisstopo.admin.ch/de/hoehenmodell-swissalti3d, last access: 2024-03-13, 2018.

swisstopo: Swiss Map Raster- Produktdokumentation, URL https://www.swisstopo.admin.ch/de/landeskarte-swiss-map-raster-25, last access: 2024-03-13, 2020a.

swisstopo: SWISSIMAGE- Das digitale Orthofotomosaik der Schweiz, URL https://www.swisstopo.admin.ch/de/orthobilder-swissimage-10-cm, last access: 2024-03-13, 2020b.

Wilhelm, C., Wiesinger, T., Bründl, M., and Ammann, W.: The Avalanche Winter 1999 in Switzerland - An Overview, in: Proceedings of the 2000 International Snow Science Workshop, October 1-6, Big Sky, Montana, pp. 487–494, URL https://arc.lib.montana.edu/snow-science/objects/issw-2000-487-494.pdf, last access: 2024-07-25, 2000.

Zweifel, B., Lucas, C., Hafner, E. D., Techel, F., Marty, C., and Stucki, T.: Schnee und Lawinen in den Schweizer Alpen. Hydrologisches Jahr 2018/19, vol. 86 of *WSL Berichte*, WSL-Institut für Schnee- und Lawinenforschung SLF; Eidg. Forschungsanstalt für Wald, Schnee und Landschaft WSL, Davos; Birmensdorf, URL https://www.dora.lib4ri.ch/wsl/islandora/object/wsl%3A22232, last access: 2024-02-27, 2019.